

GTL-1 Irradiation Summary Report

D. M. Perez
G. S. Chang
N. E. Woolstenhulme
D. M. Wachs

January 2012



The INL is a U.S. Department of Energy National Laboratory
operated by Battelle Energy Alliance

INL/EXT-10-20546

GTL-1 Irradiation Summary Report

**D. M. Perez
G. S. Chang
N. E. Woolstenhulme
D. M. Wachs**

January 2012

**Idaho National Laboratory
Idaho Falls, Idaho 83415**

<http://www.inl.gov>

**Prepared for the
U.S. Department of Energy
Office of National Nuclear Security Administration
Under DOE Idaho Operations Office
Contract DE-AC07-05ID14517**

DISCLAIMER

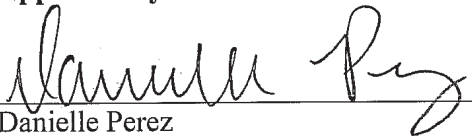
This information was prepared as an account of work sponsored by an agency of the U.S. Government. Neither the U.S. Government nor any agency thereof, nor any of their employees, makes any warranty, expressed or implied, or assumes any legal liability or responsibility for the accuracy, completeness, or usefulness, of any information, apparatus, product, or process disclosed, or represents that its use would not infringe privately owned rights. References herein to any specific commercial product, process, or service by trade name, trade mark, manufacturer, or otherwise, does not necessarily constitute or imply its endorsement, recommendation, or favoring by the U.S. Government or any agency thereof. The views and opinions of authors expressed herein do not necessarily state or reflect those of the U.S. Government or any agency thereof.

GTL-1 Irradiation Summary Report

INL/EXT-10-20546

January 2012

Approved by:



Danielle Perez
Neutronic Analyst

1/31/2012

Date


Daniel M Wachs
Principle Investigator

January 31, 2012

Date


Bruce Nielson
Experiment Manager

1/31/2012

Date

SUMMARY

The primary objective of the Gas Test Loop (GTL-1) miniplate experiment is to confirm acceptable performance of high-density (i.e., 4.8 g-U/cm³) U3Si2/Al dispersion fuel plates clad in Al-6061 and irradiated under the relatively aggressive Booster Fast Flux Loop (BFFL) booster fuel conditions, namely a peak plate surface heat flux of 450 W/cm². As secondary objectives, several design and fabrication variations were included in the test matrix that may have the potential to improve the high-heat flux, high-temperature performance of the base fuel plate design.^{1, 2}

The following report summarizes the life of the GTL-1 experiment through end of irradiation, including as-run neutronic analysis, thermal analysis and hydraulic testing results.

CONTENTS

SUMMARY	iii
ACRONYMS	vi
1. EXPERIMENT SUMMARY	1
2. CONSTITUENT MASS, MASS DENSITIES AND ATOM DENSITIES	3
3. EXPERIMENT HARDWARE.....	4
4. IRRADIATION HISTORY.....	7
5. AS-RUN NUCLEAR ANALYSIS.....	9
5.1 Physics analysis.....	9
5.2 Gradients	13
6. HYDRAULIC TESTING.....	18
7. AS-RUN THERMAL ANALYSIS	19
7.1 Coolant Temperature as a Function of Location.....	20
7.2 Plate Surface Temperatures.....	22
8. REFERENCES.....	24
Appendix A Individual Plate Power and Burnup.....	25

FIGURES

Figure 1. GTL-1 miniplate irradiation assembly (DWG 600448).	5
Figure 2. GTL-1 fuel miniplate (DWG 637215).....	6
Figure 3. GTL-1 capsule assembly.	7
Figure 4. GTL-1 capsule cross section.....	7
Figure 5. Hourly lobe power history for ATR Cycle 143A.	8
Figure 6. Transverse L2AR fission rate gradient for 26 nodes. ⁵	16
Figure 7. Axial L2AR fission rate gradient for 26 nodes. ⁵	17
Figure 8. GTL-1 coolant channel temperature along the test assembly for Cycle 143A at 18 EFPD.	20
Figure 9. GTL-1 coolant channel temperature along the test assembly for Cycle 143A at 36 EFPD.	21
Figure 10. GTL-1 coolant channel temperature along the test assembly for Cycle 143A at 48.9 EFPD.	21

TABLES

Table 1. GTL-1 experiment matrix.....	2
Table 2. As-built constituent mass, mass density and atom density for the GTL-1 miniplates. ²	3
Table 3. GTL-1 miniplate experiment hardware.....	4
Table 4. ATR irradiation history for the GTL-1 experiment. ⁵	8
Table 5. Cycle break down.	9
Table 6. GTL-1 fuel compact and processed fuel meat densities with the constituent as-built masses ⁴	10
Table 7. BOC as-run GTL-1 calculated fission heating rates and U-235 burnup. ⁵	11
Table 8. As-Run GTL-1 calculated fission heat rates and U-235 burnup at 18 EFPD. ⁵	11
Table 9. As-Run GTL-1 calculated fission heat rates and U-235 burnup at 36 EFPD. ⁵	12
Table 10. EOC as-run GTL-1 calculated fission heat rates and U-235 burnup (48.9 EFPD). ⁵	12
Table 11. Fission rate L2AR in the miniplate fuel zone transverse direction for 26 nodes.	14
Table 12. Fission rate L2AR in the miniplate fuel zone axial direction for 26 nodes.	15
Table 13. Loss coefficients for the GTL-1 irradiation test vehicle components. ⁶	18
Table 14. GTL-1 average, maximum and minimum plate surface temperatures for Cycle 143A at 18 EFPD.	22
Table 15. GTL-1 average, maximum and minimum plate surface temperatures for Cycle 143A at 36 EFPD.	22
Table 16. GTL-1 average, maximum and minimum plate surface temperatures for Cycle 143A at 48.9 EFPD.	23

ACRONYMS

Al	aluminum
ATR	Advanced Test Reactor
ATRC	Advanced Test Reactor Critical
BFFL	Booster Fast Flux Loop
BOC	beginning of cycle
DAS	Data acquisition system
EFPD	effective full-power day
GTL	Gas Test Loop
L2AR	local-to-average ratio
MCNP	Monte Carlo Neutral Particle
RERTR	Reduced Enrichment Research and Test Reactor
Si	silicon
SFT	South Flux Trap
U	uranium

GTL-1 Irradiation Summary Report

1. EXPERIMENT SUMMARY

The primary objective of the Gas Test Loop (GTL-1) miniplate experiment is to confirm acceptable performance of high-density (i.e., 4.8 g-U/cm³) U₃Si₂/Al dispersion fuel plates clad in Al-6061 and irradiated under the relatively aggressive Booster Fast Flux Loop (BFFL) booster fuel conditions, namely a peak plate surface heat flux of 450 W/cm². Additionally, miniplates operating at heat fluxes above 450 W/cm² and up to as high as 600 W/cm² were tested to demonstrate that a significant performance margin above this nominal, as-designed surface heat flux exists for the BFFL booster fuel elements. As secondary objectives, several design and fabrication variations were included in the test matrix that may have the potential to improve the high-heat flux, high-temperature performance of the base fuel plate design.^{1,2}

The nominal design of the GTL-1 fuel miniplates was based on the common Reduced Enrichment for Research and Test Reactor (RERTR) miniplate designs for the Advanced Test Reactor (ATR) with modified thickness dimensions for both the cladding and fuel meat. The GTL-1 miniplates are comprised of ground 25% enriched (U-235) Silicide fuel powder clad in aluminum (U₃Si₂/Al).³

The GTL-1 test assembly holds four capsules (designated as A, B, C, and D) with A at the top of the assembly and D at the bottom. Each capsule has two levels with two plates per level for a total of four plate positions per capsule and 16 plate positions per assembly. Within each capsule the four plates are azimuthally designated as 1, 2 in the upper level and 3, 4 in the lower level. The loading diagram for the GTL-1 experiment matrix is shown in Table 1.

Table 1. GTL-1 experiment matrix.

GTL-1 Matrix		
Capsule A	A1 Standard Powder Standard Prefilm US06C	A2 Standard Powder Modified Prefilm US15DM
	A3 Standard Powder Standard Prefilm US03HS	A4 Standard Powder Standard Prefilm US11GS
Capsule B	B1 Standard Powder Standard Prefilm US04GS	B2 No Fines Powder Standard Prefilm UN01FS
	B3 Standard Powder Standard Prefilm US02FS	B4 Annealed Powder Standard Prefilm UA01FS
Capsule C	C1 Standard Powder Standard Prefilm US07FS	C2 Standard Powder Modified Prefilm US16DM
	C3 Standard Powder Standard Prefilm US08CS	C4 Standard Powder Standard Prefilm US14DS
Capsule D	D1 Standard Powder Standard Prefilm US09GS	D2 No Fines Powder Standard Prefilm UN03ES
	D3 Standard Powder Standard Prefilm US13GS	D4 Standard Powder Modified Prefilm US17GM

2. CONSTITUENT MASS, MASS DENSITIES AND ATOM DENSITIES

Table 2. As-built constituent mass, mass density and atom density for the GTL-1 miniplates.²

Plate No.	Plate ID	Constituent Mass (g)			Fuel Volume (cc)	Constituent Mass Density (g/cc)			Constituent Atom Density (atom/barn-cm)		
		U-235	Total U	Si	Al	Total _U	Si	Al	U-235	U-238	
A-1	US06CS	1.706	6.655	0.936	2.278	1.603	1.064	4.150	0.584	1.421	2.73E-03
A-2	US15DM	1.705	6.652	0.935	2.279	1.603	1.063	4.148	0.583	1.421	2.72E-03
A-3	US03HS	1.695	6.613	0.930	2.265	1.630	1.040	4.056	0.570	1.389	2.66E-03
A-4	US11GS	1.707	6.659	0.937	2.280	1.610	1.060	4.135	0.582	1.416	2.72E-03
B-1	US04GS	1.672	6.520	0.917	2.233	1.570	1.065	4.153	0.584	1.422	2.73E-03
B-2	UN01ES	1.704	6.644	0.934	2.274	1.610	1.058	4.126	0.580	1.412	2.71E-03
B-3	US02FS	1.696	6.615	0.930	2.266	1.610	1.053	4.108	0.578	1.407	2.70E-03
B-4	UA01FS	1.705	6.651	0.935	2.278	1.610	1.059	4.130	0.581	1.415	2.71E-03
C-1	US07FS	1.708	6.644	0.937	2.283	1.617	1.056	4.109	0.580	1.412	2.71E-03
C-2	US16DM	1.705	6.652	0.936	2.277	1.603	1.063	4.148	0.583	1.420	2.72E-03
C-3	US08CS	1.703	6.644	0.934	2.275	1.603	1.062	4.144	0.583	1.419	2.72E-03
C-4	US14DS	1.707	6.658	0.936	2.280	1.597	1.069	4.170	0.586	1.428	2.74E-03
D-1	US09FS	1.708	6.662	0.937	2.282	1.610	1.061	4.137	0.582	1.417	2.72E-03
D-2	UN03ES	1.709	6.664	0.937	2.281	1.617	1.057	4.121	0.580	1.411	2.71E-03
D-3	US13GS	1.707	6.659	0.937	2.279	1.617	1.056	4.118	0.579	1.409	2.70E-03
D-4	US17GM	1.705	6.651	0.935	2.277	1.603	1.063	4.148	0.583	1.420	2.72E-03
											7.80E-03
											3.17E-02

3. EXPERIMENT HARDWARE

The GTL-1 experiment hardware is similar to that of the RERTR miniplate experiments. The experiment hardware differs slightly from the RERTR miniplate experiments due to the thicker plates and the need for more coolant flow through the capsules. The list of drawings for the hardware used for the GTL-1 experiment is shown in Table 3.³

Table 3. GTL-1 miniplate experiment hardware.

Drawing Number	Drawing Title
DWG-600310	ATR/ATRC BFFL (GTL-1) Miniplate Adapter Assemblies
DWG-600418	ATR/ATRC BFFL (GTL-1) Miniplate SFT Adapter Back-up Assemblies
DWG-600420	ATR BFFL (GTL-1) Miniplate Inner Basket Lift Assemblies and Details
DWG-600447	ATR/ATRC BFFL (GTL-1) Miniplate Modified Large B-Position Basket Detail
DWG-600448	ATR BFFL (GTL-1) Miniplate Irradiation Assembly
DWG-630233	ATR Large B-Position Basket
DWG-630231	ATR Top Spacer Assembly
DWG-630225	ATR Upper Spacer Assembly
DWG-630229	ATR Bottom Spacer Assembly
DWG-637210	GTL Mini-Plate Capsule Assembly
DWG-637212	Capsule. GTL
DWG-637213	Capsule Cap
DWG-637215	Fuel Plate, 0.040 in. Thick Fuel

The GTL-1 miniplate irradiation assembly, (see Figure 1) shows the main components of the test assembly, which include the bottom spacer, upper and top spacers, experiment capsules and basket. The bottom spacer elevates the experiment capsules to the correct location in the core. The upper and top spacers allow the operators to assure that the experiment is seated fully into the basket. All spacers are similar to the capsule design except the spacers do not have the grooves for the plates. The capsules hold the fuel plates; a capsule cap is welded onto the top of the capsule to keep the plates from sliding out during handling and irradiation. The fuel plate drawings plates (DWG-637215) and GTL-1 miniplate capsule assembly are shown in Figure 2 and Figure 3, respectively. Each capsule has a notch at the top and a groove at the bottom which allow the capsules to stack and align properly into the core. The basket holds the test assembly in the reactor during irradiation, the notches on the outer wall allow for bypass coolant flow to cool the outer wall. The basket has two guide bars on the inside wall to guide the assembly into the baskets.

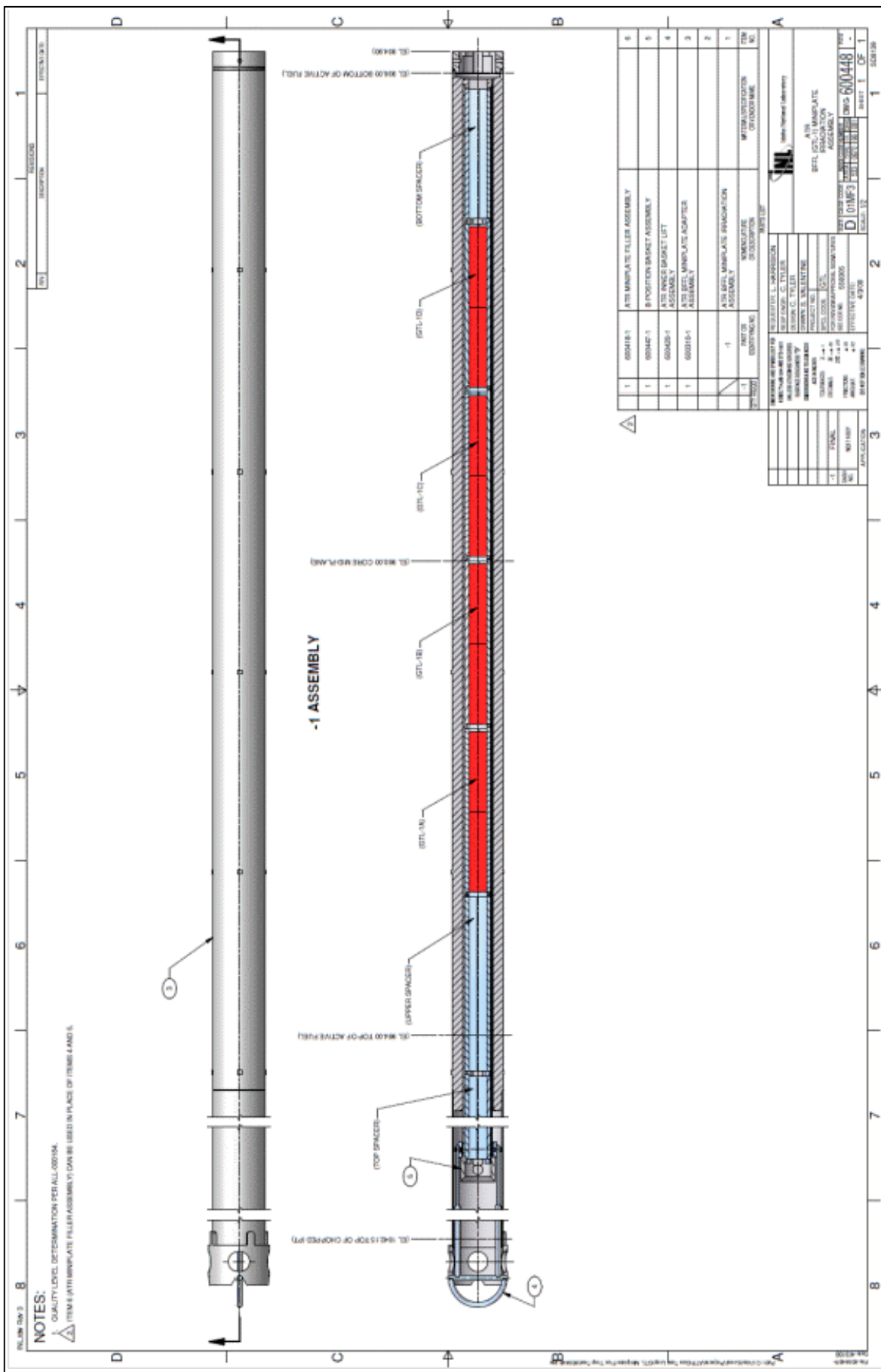


Figure 1. GTL-1 miniplate irradiation assembly (DWG 600448).

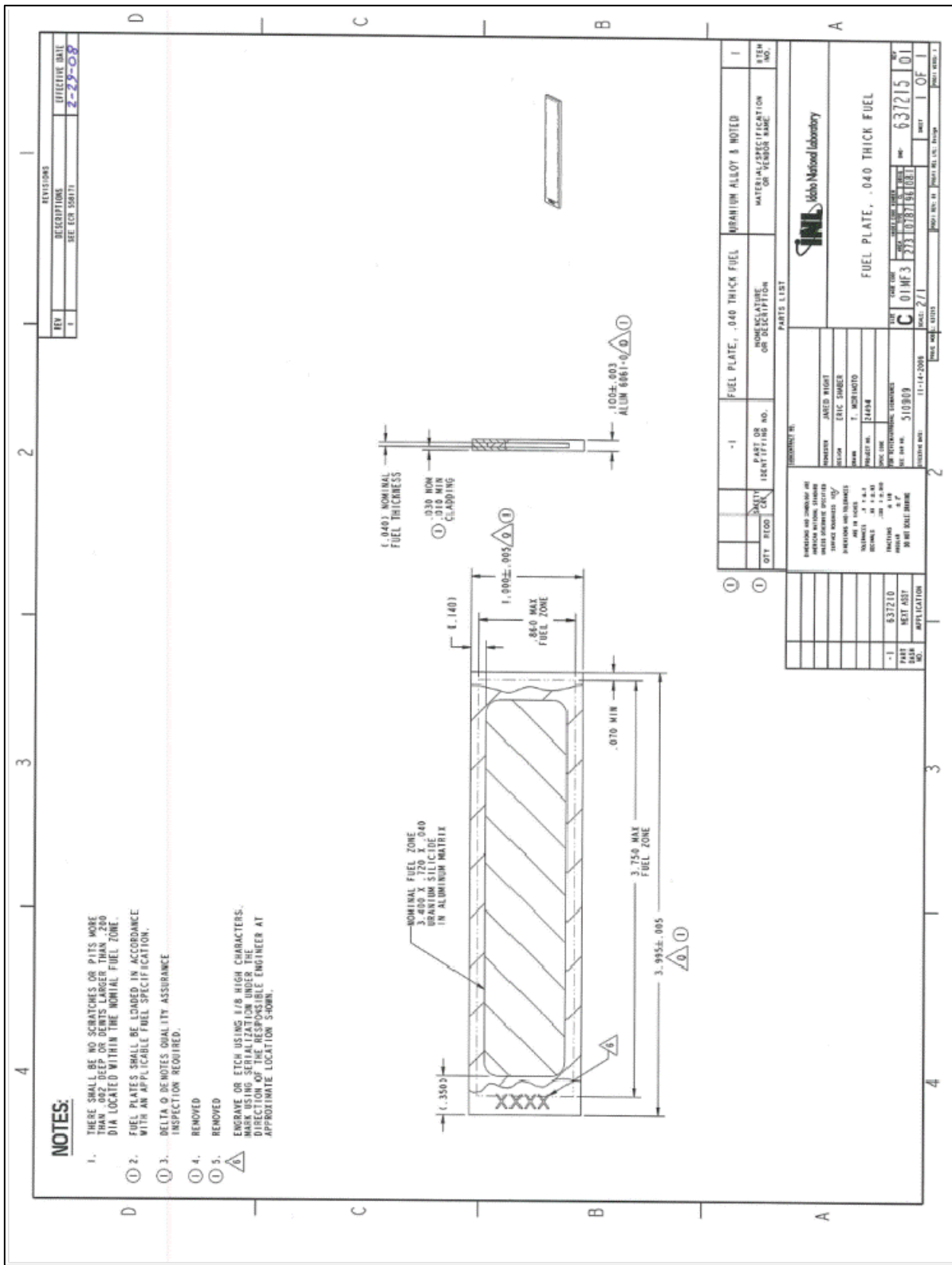


Figure 2. GTL-1 fuel miniplate (DWG 637215).



Figure 3. GTL-1 capsule assembly.

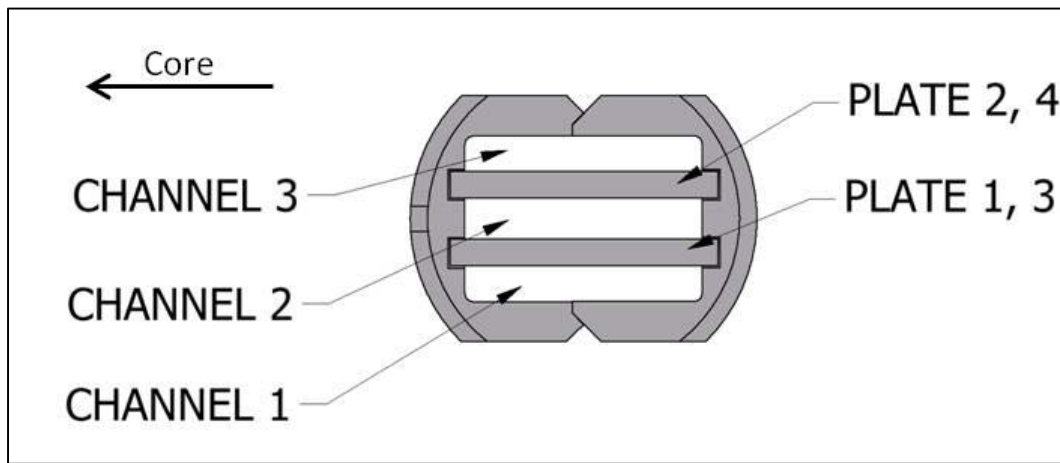


Figure 4. GTL-1 capsule cross section.

4. IRRADIATION HISTORY

The GTL-1 test assembly was irradiated during ATR Cycle 143A in the South Flux Trap (SFT) position. The power of this position is the average of the SW, C, and SE lobe powers, $S = (SW + C + SE)/3$. Cycle 143A ran for 48.9 Effective Full Power Days (EFPD) at 25.4 MW. Cycle 143A began September 24, 2008 and ended December 6, 2008 with two cycle interruptions. The first cycle interruption was October 16, 2008–November 5, 2008 (20 days) and the second cycle interruption was from November 21, 2008–November 26, 2008 (5 days) for a total of 25 mid-cycle SCRAM decay days. This information is tabulated in Table 4.

Table 4. ATR irradiation history for the GTL-1 experiment.⁵

ATR Cycle	Test ID	Capsules Irradiated	Dates Irradiated	Cycle EFPD	Mid-Cycle Scram Decay Days	Post-Cycle Decay Days	South Lobe Source Power (MW)
143A	GTL-1	A,B,C,D	10/16/2008 – 11/26/2008	48.9	25	17	25.4

The Power history for Cycle 143A is obtained as an ATR Surveillance Report from the ATR Data Acquisition System (DAS). The plot of each lobe power on an hourly basis is shown in Figure 5.

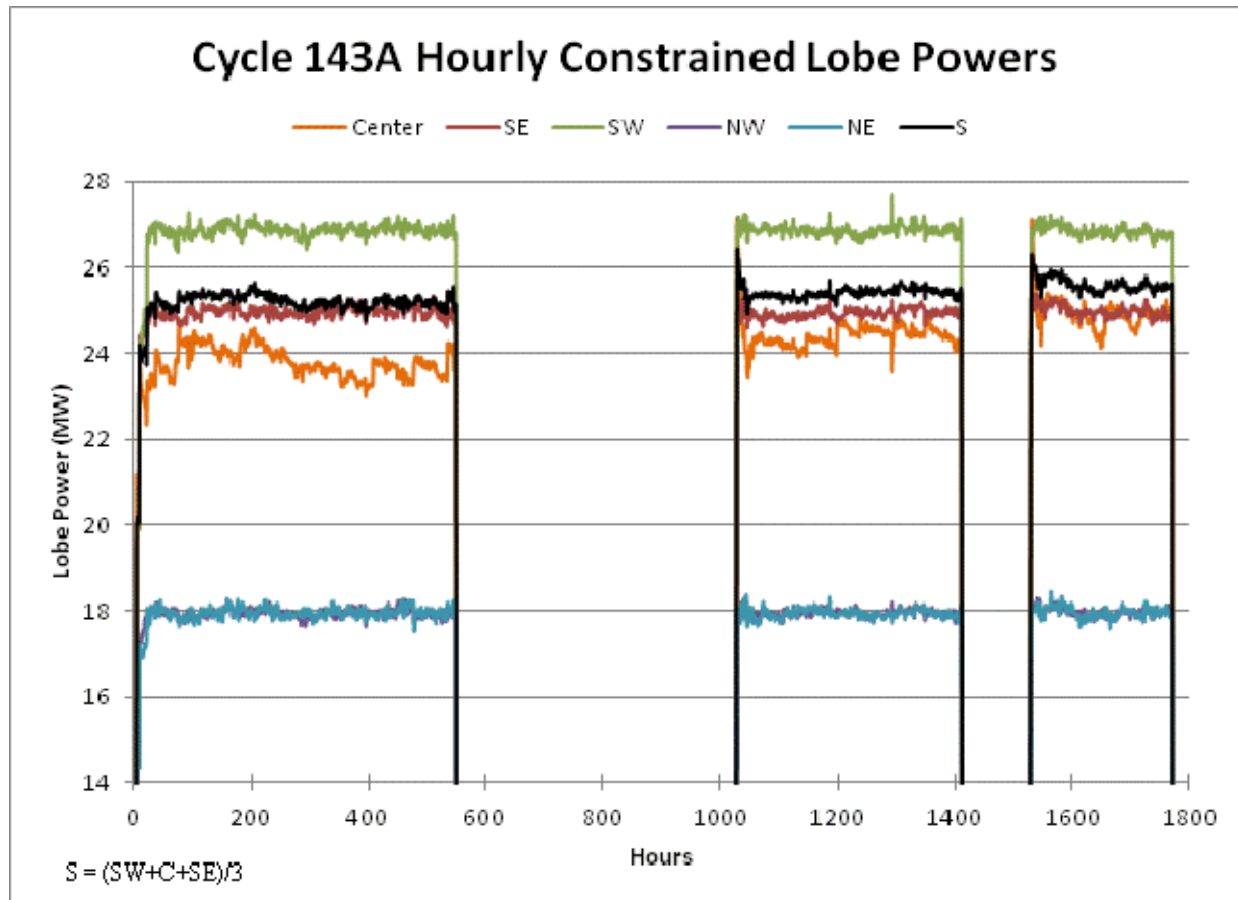


Figure 5. Hourly lobe power history for ATR Cycle 143A.

5. AS-RUN NUCLEAR ANALYSIS

5.1 Physics analysis

The as-run calculations were performed using the irradiation history in Table 4 and the Monte Carlo N-Particle (MCNP) transport code. The calculated as-run fission heat rates and as-run U-235 burnup results for the fueled miniplates reported have an uncertainty band (1σ) of 2.5%.⁵ The time intervals used to calculate average plate power and burnup is shown in Table 5.

Table 5. Cycle break down.

Time Interval	143A (Days)
01	1.0e-4
02	18.0
03	18.0
04	12.9
05	1.0e-4
EFPD	48.9

The MCNP model contained fuel meat densities based upon the measured volume of the fuel compact before undergoing the rolling fabrication process. Porosity within the fuel compact is reduced during the rolling fabrication process, thus increasing the actual density of the processed fuel meat. Therefore, the MCNP-modeled fuel meat densities are less than the actual processed fuel meat densities. To better represent the processed fuel meat densities, the rule of mixtures is used to calculate the density based upon the as-built masses and theoretical densities for U_3Si_2 and Al matrix. The rule of mixtures is given by equation (1). These corrected densities for the processed fuel meat were used to update the MCNP-calculated fission power density (W/cc) and heat flux (W/cm²). The as-built masses and calculated densities for the fuel compacts and the processed fuel meat are tabulated in Table 6.

$$\rho_{processed\ fuel\ meat} = \frac{(mass_{fuel\ powder} + mass_{Al\ powder})}{\left(\frac{mass_{fuel\ powder}}{\rho_{theoretical\ (fuel\ powder)}} + \frac{mass_{Al\ powder}}{\rho_{theoretical\ (Al\ powder)}} \right)} \quad (1)$$

The corrected fission heat rates at the beginning of cycle (BOC) are shown in Table 7. Table 8 through Table 10 contain the fission heat rates and U-235 burnup for 18 EFPD, 36 EFPD, and 48.9 EFPD, respectively. The individual plate power and burnup (fission density) are shown in Appendix A

Table 6. GTL-1 fuel compact and processed fuel meat densities with the constituent as-built masses⁴.

Plate Position	Plate ID	Measured Fuel Powder (U & Si) Mass (g)	Measured Al Powder Mass (g)	Calculated Fuel Compact Density (g/cc)	Calculated Processed Fuel Meat Density (g/cc)
A-1	US06CS	7.591	2.278	6.16	6.732
A-2	US15DM	7.587	2.279	6.15	6.730
A-3	US03HS	7.543	2.265	6.02	6.731
A-4	US11GS	7.596	2.280	6.13	6.732
B-1	US04GS	7.437	2.233	6.16	6.731
B-2	UN01ES	7.579	2.274	6.12	6.733
B-3	US02FS	7.545	2.266	6.09	6.730
B-4	UA01FS	7.587	2.278	6.13	6.731
C-1	US07FS	7.601	2.283	6.10	6.730
C-2	US16DM	7.588	2.277	6.15	6.732
C-3	US08CS	7.579	2.275	6.14	6.732
C-4	US14DS	7.595	2.280	6.19	6.731
D-1	US09FS	7.599	2.282	6.14	6.731
D-2	UN03ES	7.602	2.281	6.11	6.733
D-3	US13GS	7.596	2.279	6.11	6.733
D-4	US17GM	7.586	2.277	6.15	6.732

Table 7. BOC as-run GTL-1 calculated fission heating rates and U-235 burnup.⁵

Plate No.	Plate ID	Calculated Processed Fuel Meat Density (g/cm ³)	Fission Heat Rate (W/g)	Fission Power Density (W/cm ³)	Heat Flux (W/cm ²)
A-1	US06CS	6.732	1231.82	8292.96	421.28
A-2	US15DM	6.730	1236.26	8320.12	422.66
A-3	US03HS	6.731	1535.49	10335.21	525.03
A-4	US11GS	6.732	1531.27	10308.20	523.66
B-1	US04GS	6.731	1789.03	12042.03	611.74
B-2	UN01ES	6.733	1790.22	12053.02	612.29
B-3	US02FS	6.730	1902.36	12803.77	650.43
B-4	UA01FS	6.731	1899.59	12786.28	649.54
C-1	US07FS	6.730	1920.01	12922.22	656.45
C-2	US16DM	6.732	1924.17	12954.30	658.08
C-3	US08CS	6.732	1833.64	12343.52	627.05
C-4	US14DS	6.731	1837.16	12366.81	628.23
D-1	US09FS	6.731	1636.48	11014.63	559.54
D-2	UN03ES	6.733	1639.38	11037.31	560.70
D-3	US13GS	6.733	1389.15	9352.92	475.13
D-4	US17GM	6.732	1386.41	9333.00	474.12

Table 8. As-Run GTL-1 calculated fission heat rates and U-235 burnup at 18 EFPD.⁵

Plate No.	Plate ID	Calculated Processed Fuel Meat Density (g/cm ³)	Fission Heat Rate (W/g)	Fission Power Density (W/cm ³)	Fission Heat Flux (W/cm ²)	U-235 Burnup $\Delta U_{235}/U_{235_0}$ (%)	Fission Density (fission/cm ³)
A-1	US06CS	6.732	1153.75	7767.42	394.58	16.07%	4.02E+20
A-2	US15DM	6.730	1153.28	7761.65	394.29	16.12%	4.03E+20
A-3	US03HS	6.731	1382.52	9305.58	472.72	19.56%	4.89E+20
A-4	US11GS	6.732	1383.52	9313.57	473.13	19.55%	4.98E+20
B-1	US04GS	6.731	1553.58	10457.23	531.23	22.43%	5.84E+20
B-2	UN01ES	6.733	1557.52	10486.36	532.71	22.43%	5.80E+20
B-3	US02FS	6.730	1623.45	10926.58	555.07	23.64%	6.14E+20
B-4	UA01FS	6.731	1622.89	10923.83	554.93	23.63%	6.17E+20
C-1	US07FS	6.730	1634.59	11001.25	558.86	23.84%	6.21E+20
C-2	US16DM	6.732	1633.82	10999.51	558.78	23.90%	6.27E+20
C-3	US08CS	6.732	1581.58	10646.69	540.85	22.93%	5.97E+20
C-4	US14DS	6.731	1583.31	10658.03	541.43	22.96%	6.02E+20
D-1	US09FS	6.731	1448.00	9746.03	495.10	20.75%	5.32E+20
D-2	UN03ES	6.733	1450.39	9764.90	496.06	20.75%	5.31E+20
D-3	US13GS	6.733	1271.45	8560.41	434.87	17.89%	4.50E+20
D-4	US17GM	6.732	1266.08	8523.02	432.97	17.88%	4.52E+20

Table 9. As-Run GTL-1 calculated fission heat rates and U-235 burnup at 36 EFPD.⁵

Plate No.	Plate ID	Calculated Processed Fuel Meat Density (g/cm ³)	Fission Heat Rate (W/g)	Fission Power Density (W/cm ³)	Fission Heat Flux (W/cm ²)	U-235 Burnup $\Delta U_{235}/U_{235_0}$ (%)	Fission Density (fission/cm ³)
A-1	US06CS	6.732	1079.66	7268.57	369.24	30.63%	7.74E+20
A-2	US15DM	6.730	1086.55	7312.52	371.48	30.69%	7.75E+20
A-3	US03HS	6.731	1253.13	8434.62	428.48	36.52%	9.23E+20
A-4	US11GS	6.732	1250.91	8420.86	427.78	36.49%	9.40E+20
B-1	US04GS	6.731	1353.10	9107.78	462.68	41.00%	1.08E+21
B-2	UN01ES	6.733	1353.63	9113.58	462.97	41.02%	1.08E+21
B-3	US02FS	6.730	1393.90	9381.58	476.58	42.87%	1.13E+21
B-4	UA01FS	6.731	1391.82	9368.43	475.92	42.87%	1.13E+21
C-1	US07FS	6.730	1404.18	9450.54	480.09	43.13%	1.14E+21
C-2	US16DM	6.732	1399.23	9420.16	478.54	43.21%	1.15E+21
C-3	US08CS	6.732	1372.99	9242.55	469.52	41.79%	1.10E+21
C-4	US14DS	6.731	1374.37	9251.54	469.98	41.80%	1.11E+21
D-1	US09FS	6.731	1298.40	8739.11	443.95	38.30%	9.95E+20
D-2	UN03ES	6.733	1303.77	8777.77	445.91	38.37%	9.92E+20
D-3	US13GS	6.733	1177.98	7931.12	402.90	33.72%	8.56E+20
D-4	US17GM	6.732	1179.01	7936.87	403.19	33.66%	8.59E+20

Table 10. EOC as-run GTL-1 calculated fission heat rates and U-235 burnup (48.9 EFPD).⁵

Plate No.	Plate ID	Calculated Processed Fuel Meat Density (g/cm ³)	Fission Heat Rate (W/g)	Fission Power Density (W/cm ³)	Fission Heat Flux (W/cm ²)	U-235 Burnup $\Delta U_{235}/U_{235_0}$ (%)	Fission Density (fission/cm ³)
A-1	US06CS	6.732	997.36	6714.51	341.10	40.28%	1.02E+21
A-2	US15DM	6.730	1001.35	6739.18	342.35	40.38%	1.02E+21
A-3	US03HS	6.731	1128.53	7595.96	385.87	47.33%	1.20E+21
A-4	US11GS	6.732	1128.35	7595.80	385.87	47.31%	1.22E+21
B-1	US04GS	6.731	1196.70	8055.02	409.19	52.36%	1.38E+21
B-2	UN01ES	6.733	1195.25	8047.29	408.80	52.38%	1.38E+21
B-3	US02FS	6.730	1221.37	8220.41	417.60	54.46%	1.44E+21
B-4	UA01FS	6.731	1219.28	8207.10	416.92	54.44%	1.44E+21
C-1	US07FS	6.730	1227.20	8259.42	419.58	54.77%	1.45E+21
C-2	US16DM	6.732	1225.04	8247.47	418.97	54.81%	1.46E+21
C-3	US08CS	6.732	1206.66	8122.84	412.64	53.29%	1.41E+21
C-4	US14DS	6.731	1208.91	8137.79	413.40	53.30%	1.42E+21
D-1	US09FS	6.731	1161.59	7818.27	397.17	49.37%	1.29E+21
D-2	UN03ES	6.733	1164.23	7838.28	398.18	49.48%	1.28E+21
D-3	US13GS	6.733	1071.93	7217.11	366.63	44.07%	1.12E+21
D-4	US17GM	6.732	1071.78	7215.03	366.52	44.02%	1.13E+21

5.2 Gradients

The MCNP-calculated power gradients in the transverse and axial directions are represented by the fission rate local-to-average ratios (L2ARs) as a function of position for eight fuel plates (one column of fuel plates [i.e., A-1, A-3, B-1, B-3, C-1, C-3, D-1, and D-3]). The calculated gradients may be used to represent the gradient for either column of fuel plates. The L2AR fission power gradients in the transverse direction for the GTL-1 fueled miniplates are shown in Table 11 and plotted in Figure 6. The L2AR fission power gradients in the axial direction for the GTL-1 fueled miniplates are shown in Table 12 and are plotted in Figure 7.⁵

Table 11. Fission rate L2AR in the miniplate fuel zone transverse direction for 26 nodes.

	Core Center Edge						Position						
	1	2	3	4	5	6	7	8	9	10	11	12	13
Plate A1/A2	1.097	1.041	1.013	1.000	0.987	0.951	0.967	0.983	0.971	0.971	0.968	0.965	0.980
Plate A3/A4	1.077	1.022	1.001	0.986	0.996	0.981	0.978	0.956	0.962	0.978	0.985	0.984	1.000
Plate B1/B2	1.067	1.016	1.010	0.998	0.988	0.972	0.973	0.983	0.986	0.977	0.964	0.963	0.975
Plate B3/B4	1.059	1.009	1.012	0.993	0.992	0.998	1.003	0.986	0.978	0.971	0.969	0.972	0.970
Plate C1/C2	1.064	0.998	0.991	0.990	0.981	0.983	0.983	0.986	0.981	0.973	0.976	0.989	0.975
Plate C3/C4	1.075	1.027	1.004	1.002	0.992	0.993	0.976	0.973	0.979	0.992	0.971	0.990	0.978
Plate D1/D2	1.077	1.017	0.991	0.983	0.995	0.978	0.970	0.981	0.978	0.978	0.971	0.988	0.994
Plate D3/D4	1.051	1.005	1.005	0.979	0.996	0.982	0.986	0.989	0.970	0.979	0.981	0.997	0.978
Outer Edge													
	14	15	16	17	18	19	20	21	22	23	24	25	26
Plate A1/A2	0.962	0.976	0.990	0.998	0.984	1.008	0.989	0.997	0.995	1.010	1.023	1.058	1.117
Plate A3/A4	0.978	0.965	0.971	0.974	0.984	0.984	1.012	1.026	1.022	1.037	1.047	1.120	
Plate B1/B2	0.978	0.979	0.978	0.966	0.987	0.986	0.992	1.010	1.019	1.020	1.031	1.060	1.119
Plate B3/B4	0.972	0.971	0.977	0.983	0.977	0.994	0.990	0.982	1.011	1.010	1.029	1.066	1.125
Plate C1/C2	0.968	0.972	0.982	0.985	0.995	0.994	1.002	1.004	1.009	1.019	1.032	1.057	1.113
Plate C3/C4	0.977	0.982	0.973	0.976	0.985	0.988	0.974	0.990	1.012	1.012	1.020	1.049	1.110
Plate D1/D2	0.981	0.976	0.981	0.987	0.983	1.000	0.997	0.992	1.017	1.026	1.047	1.119	
Plate D3/D4	0.961	0.993	0.999	0.971	0.970	0.970	0.981	0.997	1.021	1.020	1.050	1.063	1.107

Table 12. Fission rate L2AR in the miniplate fuel zone axial direction for 26 nodes.

	Top of Plate												Position				
	1	2	3	4	5	6	7	8	9	10	11	12	13				
Plate A1/A2	0.949	0.946	0.896	0.904	0.948	0.915	0.935	0.951	0.942	0.947	0.951	0.974					
Plate A3/A4	0.994	0.960	0.946	0.944	0.940	0.960	0.961	0.954	0.960	0.947	0.958	0.978					
Plate B1/B2	0.992	0.966	0.965	0.943	0.980	0.977	0.981	0.949	0.986	0.989	0.997	1.006					
Plate B3/B4	1.044	1.007	0.993	1.008	0.995	0.976	0.988	0.985	0.954	0.963	0.992	0.964					
Plate C1/C2	1.080	1.019	1.012	0.984	0.980	0.997	1.004	1.004	0.995	1.015	1.007	0.994					
Plate C3/C4	1.071	1.022	1.017	1.010	0.998	1.002	1.012	0.997	0.988	0.988	0.999	0.982					
Plate D1/D2	1.111	1.056	1.038	1.014	1.027	1.025	1.016	1.003	1.003	1.003	1.007	1.012					
Plate D3/D4	1.119	1.065	1.101	1.061	1.070	1.039	1.016	1.025	1.010	1.013	1.029	1.002					
Position																	
Bottom of Plate																	
14	1.5	16	17	18	19	20	21	22	23	24	25	26					
Plate A1/A2	1.012	0.987	1.032	1.052	1.009	1.019	1.045	1.044	1.078	1.098	1.095	1.105					
Plate A3/A4	1.017	1.006	0.990	1.013	0.996	1.007	1.030	1.050	1.033	1.035	1.067	1.094					
Plate B1/B2	1.000	0.985	0.983	1.013	1.004	1.003	1.019	1.006	1.018	1.049	1.041	1.046					
Plate B3/B4	0.986	0.978	0.986	1.008	1.001	1.001	1.011	1.015	1.002	1.005	1.022	1.049					
Plate C1/C2	0.981	0.991	0.993	0.989	0.978	0.988	1.000	0.986	0.980	0.992	0.997	1.054					
Plate C3/C4	1.006	1.001	0.979	0.993	0.976	0.985	0.994	0.963	0.979	0.985	1.009	1.070					
Plate D1/D2	0.977	0.978	0.990	0.980	0.999	0.981	0.975	0.973	0.951	0.983	0.963	0.952					
Plate D3/D4	0.984	0.971	0.980	0.949	0.971	0.969	0.970	0.959	0.936	0.933	0.940	0.982					

Transverse Fission Rate L2AR Gradients For 26 Nodes

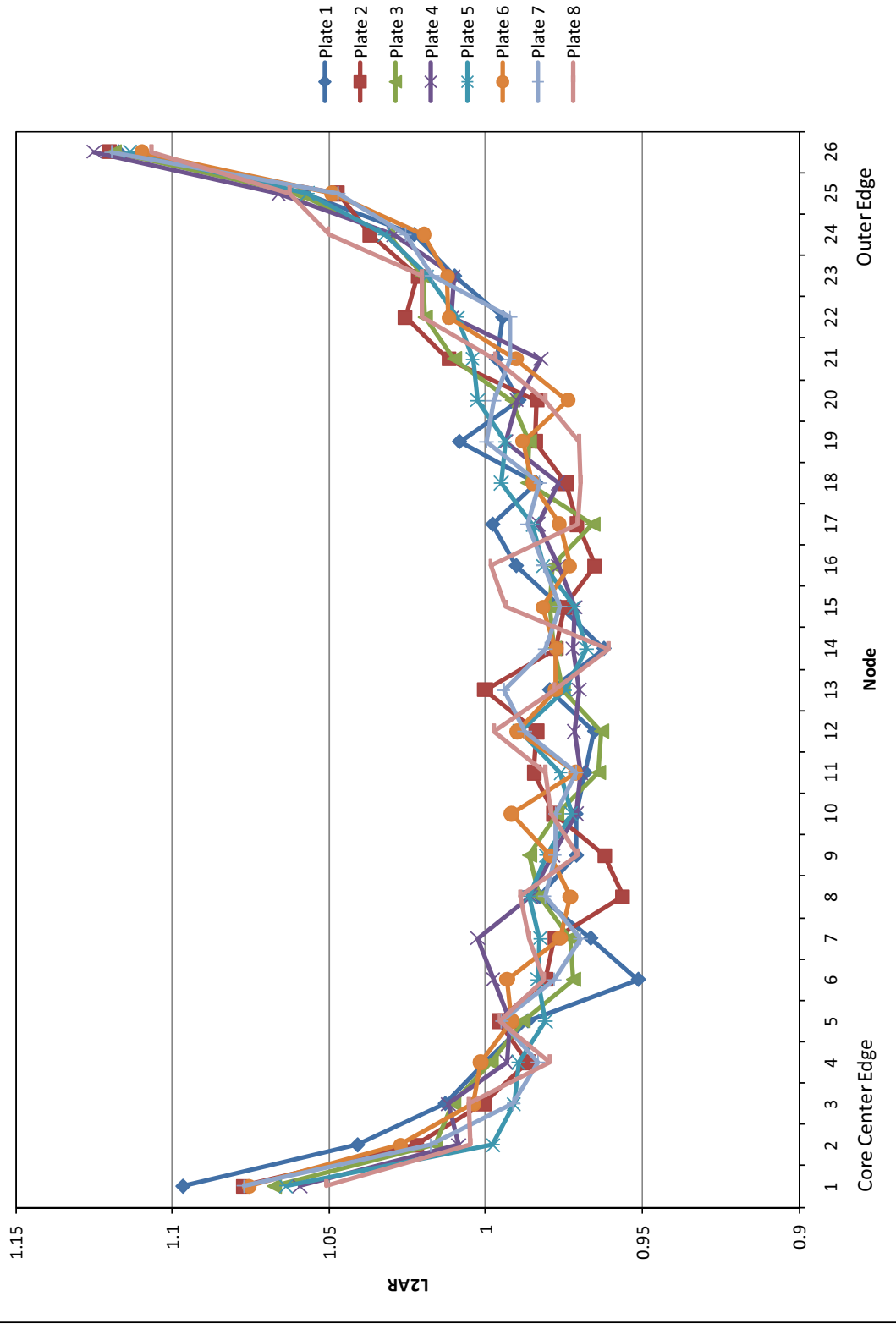


Figure 6. Transverse L2AR fission rate gradient for 26 nodes.⁵

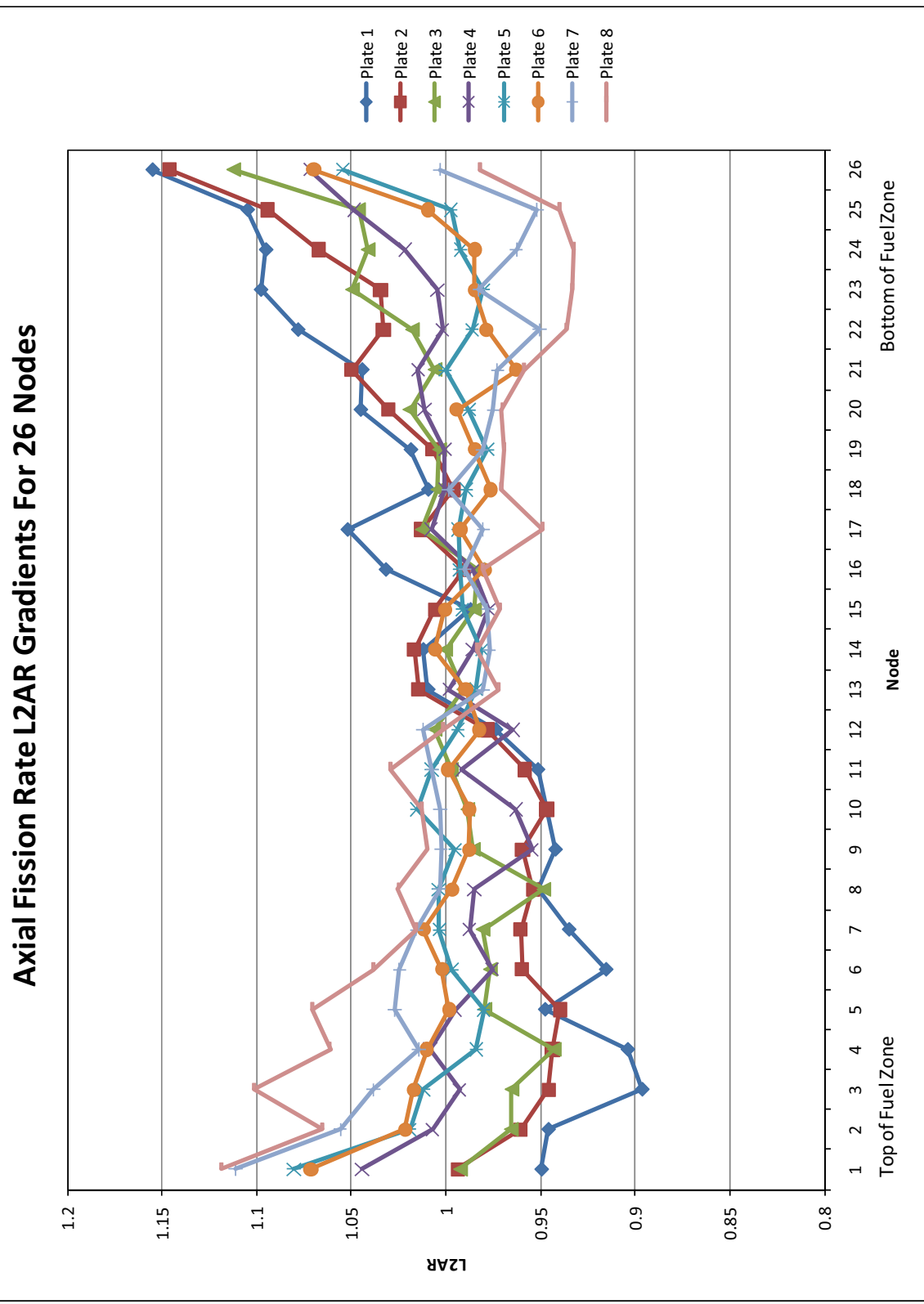


Figure 7. Axial L2AR fission rate gradient for 26 nodes.⁵

6. HYDRAULIC TESTING

Flow tests were performed to characterize the test vehicle designed to irradiate miniplates for the GTL project. The vehicle had been used for multiple flow tests for the RERTR program irradiation tests. The results of the flow tests will be used to generate high confidence estimates of the coolant flow rate required to accurately calculate the miniplate temperatures during irradiation.

The test apparatus was designed and constructed to simulate the ATR Large-B position and flow conditions. The test vehicle was fabricated such that the orifice plate could be easily interchanged (screwed on instead of welded on the test vehicle). Three orifice plate sizes were tested along with no orifice plate and with the basket exit blocked (to measure bypass flow). The results of this test are shown in Table 13.⁶

Table 13. Loss coefficients for the GTL-1 irradiation test vehicle components.⁶

Orifice Diameter (mm)	K/A ² (1/m ⁴)	ATR Coolant Flow	
		Rate (GPM)	ATR Coolant Velocity (ft/sec)
Bypass	2.8414 E 8	30.1	—
Open	8.3028 E 7	55.6	47.8
9	7.5754 E 8	17.5	15.1
8	1.8588 E 9	11.5	9.9
7	2.7422 E 9	9.5	8.2

Even though the GTL-1 experiment was irradiated in the SFT, the design parameters for the target coolant flow rate were still applicable. An insert mimicking the Large -B position was put into the SFT for irradiation of the GTL-1 experiment.

7. AS-RUN THERMAL ANALYSIS

The as-run thermal analysis was performed using the MCNP-generated heat flux calculations, the nominal coolant flow rate and as-built fuel meat thickness. The heat transfer correlation used to calculate the plate surface temperature and the coolant channel temperatures was the Petukhov heat transfer correlation⁷ (see equation (2)).

$$Nu = \frac{hD}{k} = \frac{(f_F/2)RePr}{1.07 + 12.7(f_F/2)^{1/2}(Pr^{2/3} - 1)} \left(\frac{\mu}{\mu_w} \right)^{0.14} \quad (2)$$

Where Nu is the Nusselt number, h is the heat transfer coefficient, D is the hydraulic diameter, k is the thermal conductivity, Re is the Reynolds number, Pr is the Prandtl number, f_F is the Fanning friction factor⁷ (see equation (3)), μ is the fluid dynamic viscosity at the bulk temperature and μ_w is the fluid dynamic viscosity at the wall temperature.

$$f_F = (3.64 \log_{10} Re - 3.28)^{-2} \quad (3)$$

The coolant temperature along the fuel zone of each plate (equation (4)) was analyzed at the three flow channels in the test assembly, zero mixing between capsules was assumed for these calculations, the plate surface temperature (equation (5)) was analyzed for the front and back of the plates.

$$T_{cool} = \frac{q''A}{\rho c_p Q} + T_{in} \quad (4)$$

Where q'' is the MCNP-calculated heat flux, A is the cross sectional area of the coolant channel, ρ is the density of the fluid, c_p is fluid specific heat, Q is the coolant volumetric flow rate through the given channel and T_{in} is the coolant temperature at the axial location that precedes the current axial location.

$$T_{surface} = \frac{q''}{h} + T_{cool} \quad (5)$$

7.1 Coolant Temperature as a Function of Location

The coolant temperature was analyzed at the three flow channels in the test assembly, with channel 1 at the left of the assembly; channel 2 in between the plates and channel 3 at the right of the assembly (see Figure 4). The coolant temperature was plotted as a function of location along the test assembly at each time step. These plots are shown in Figure 8 through Figure 10.

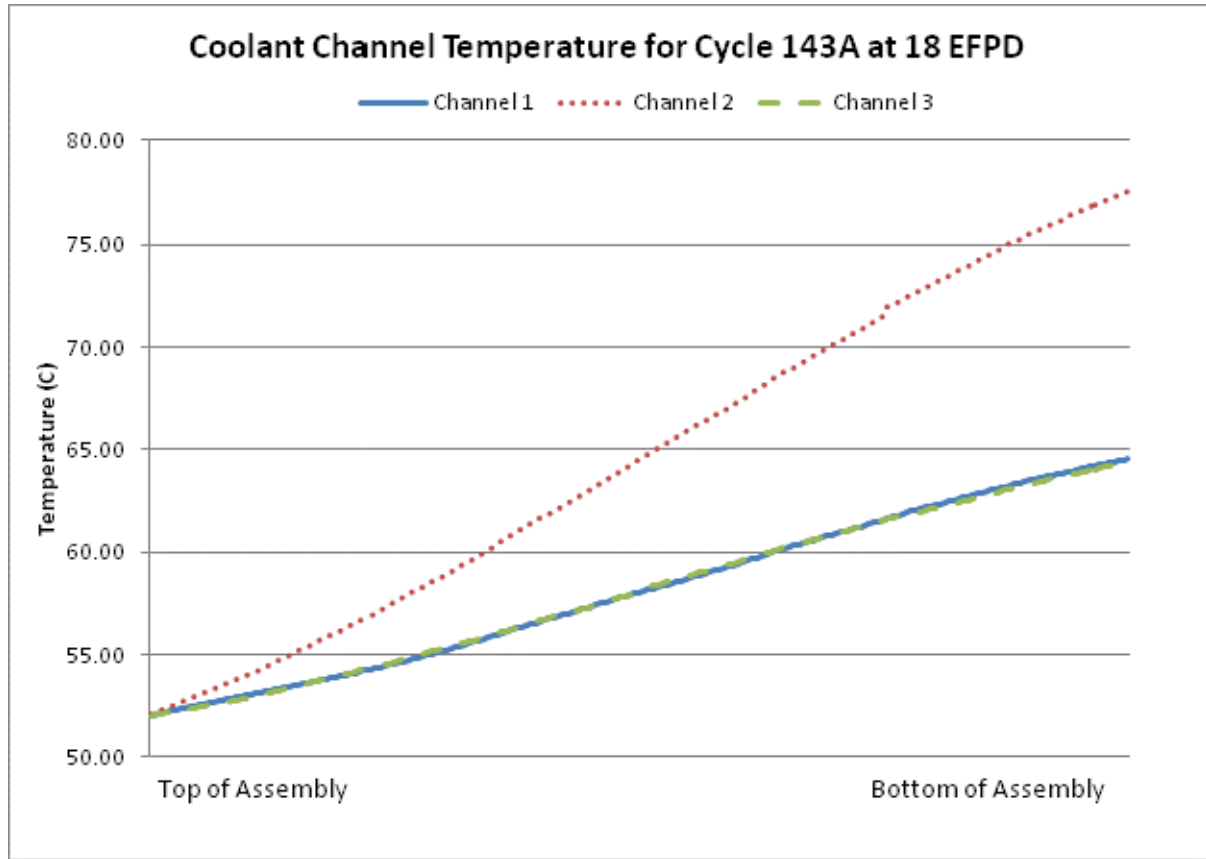


Figure 8. GTL-1 coolant channel temperature along the test assembly for Cycle 143A at 18 EFPD.

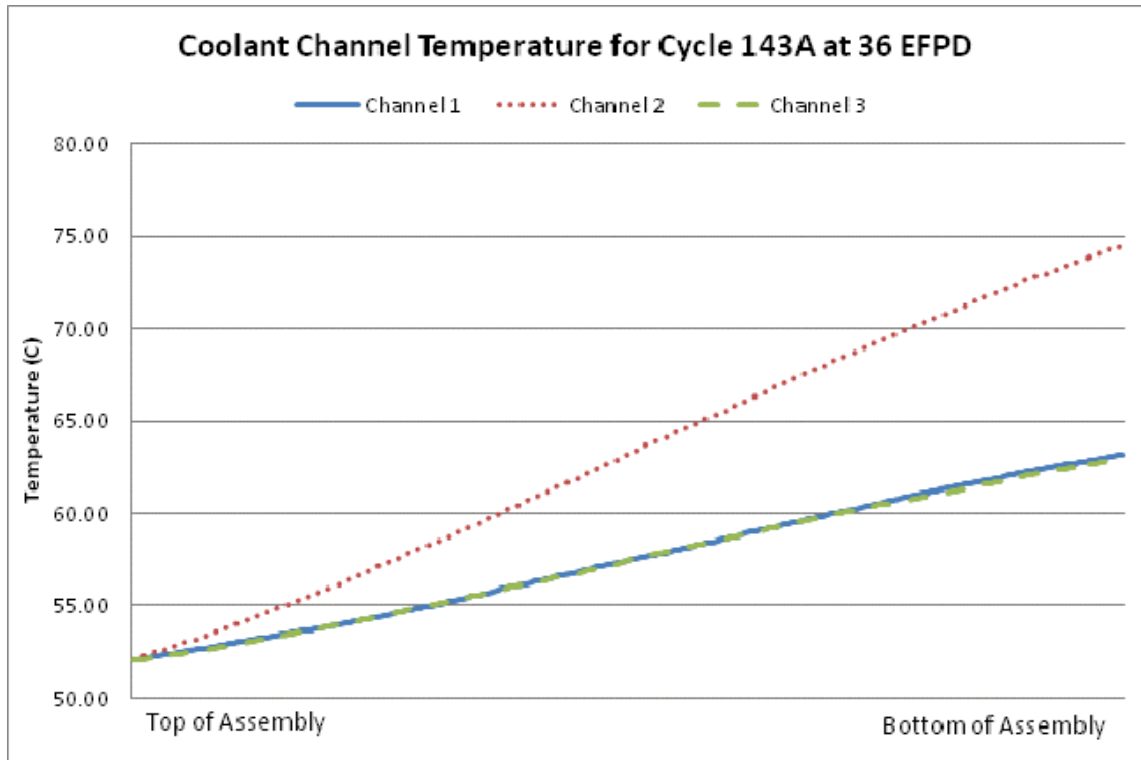


Figure 9. GTL-1 coolant channel temperature along the test assembly for Cycle 143A at 36 EFPD.

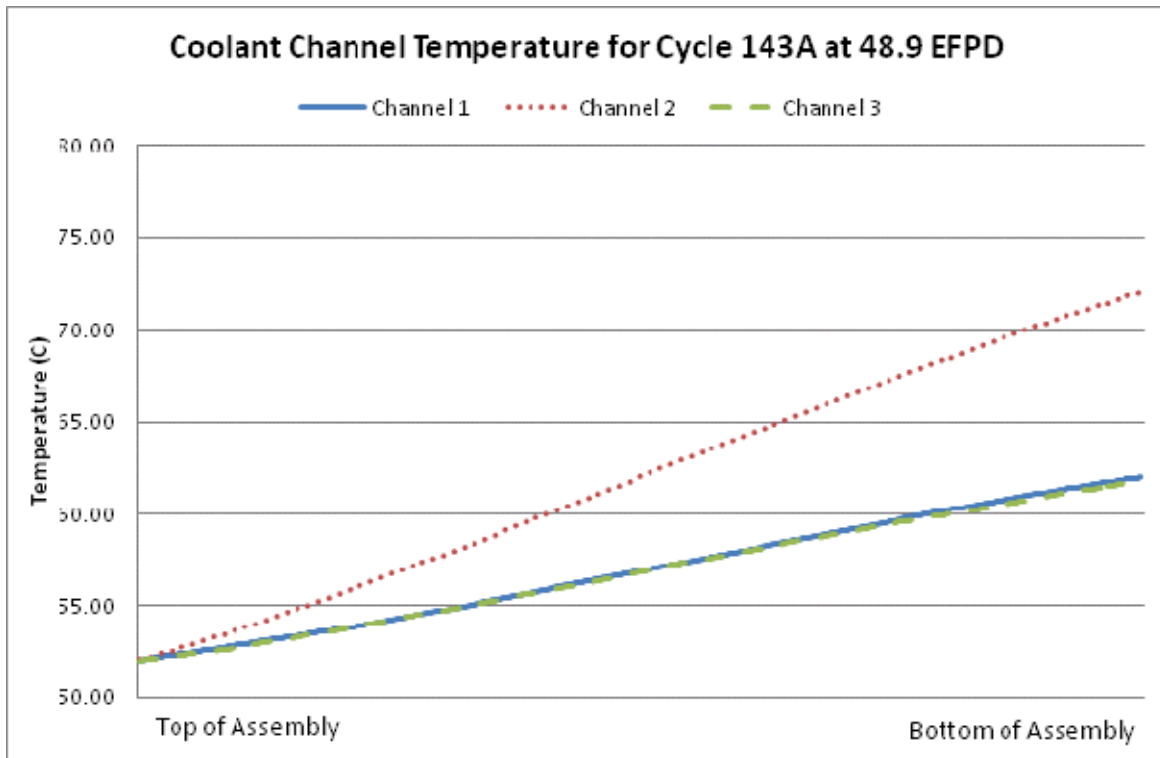


Figure 10. GTL-1 coolant channel temperature along the test assembly for Cycle 143A at 48.9 EFPD.

7.2 Plate Surface Temperatures

The average, maximum and minimum plate temperatures for each time step in Cycle 143A are provided in Table 14 through Table 16.

Table 14. GTL-1 average, maximum and minimum plate surface temperatures for Cycle 143A at 18 EFPD.

Plate Location	Plate ID	Average Temperature (C)	Maximum Temperature (C)	Minimum Temperature (C)
A1	US06C	100.06	105.85	92.52
A2	US15DM	99.81	118.65	89.27
A3	US03HS	108.05	128.69	97.65
A4	US11GS	111.16	124.74	102.61
B1	US04GS	117.27	142.47	104.56
B2	UN01FS	117.82	134.71	107.55
B3	US02FS	123.08	141.71	113.05
B4	UA01FS	122.30	138.85	109.90
C1	US07FS	125.69	147.28	110.15
C2	US16DM	124.39	147.73	109.32
C3	US08CS	124.54	139.58	114.20
C4	US14DS	125.44	138.26	116.18
D1	US09GS	123.95	144.06	106.68
D2	UN03ES	120.10	138.13	105.08
D3	US13GS	116.95	130.00	107.14
D4	US17GM	117.19	130.09	96.14

Table 15. GTL-1 average, maximum and minimum plate surface temperatures for Cycle 143A at 36 EFPD.

Plate Location	Plate ID	Average Temperature (C)	Maximum Temperature (C)	Minimum Temperature (C)
A1	US06C	97.19	102.66	90.08
A2	US15DM	96.70	115.12	86.37
A3	US03HS	103.73	114.18	93.68
A4	US11GS	105.98	118.46	98.11
B1	US04GS	111.19	132.16	94.40
B2	UN01FS	110.08	125.16	100.89
B3	US02FS	114.63	130.58	105.93
B4	UA01FS	113.83	128.84	102.99
C1	US07FS	116.42	135.59	102.72
C2	US16DM	115.16	135.77	101.85
C3	US08CS	116.00	129.40	106.74
C4	US14DS	116.77	128.18	108.50
D1	US09GS	117.00	135.12	101.35
D2	UN03ES	113.58	129.81	99.96
D3	US13GS	111.98	123.80	103.08
D4	US17GM	112.40	124.12	92.85

Table 16. GTL-1 average, maximum and minimum plate surface temperatures for Cycle 143A at 48.9 EFPD.

Plate Location	Plate ID	Average Temperature (C)	Maximum Temperature (C)	Minimum Temperature (C)
A1	US06C	93.97	99.08	87.34
A2	US15DM	93.31	110.58	83.63
A3	US03HS	99.35	115.92	89.81
A4	US11GS	101.11	112.54	93.91
B1	US04GS	104.98	123.87	93.47
B2	UN01FS	103.89	117.49	95.62
B3	US02FS	107.94	121.91	100.15
B4	UA01FS	107.16	120.81	97.51
C1	US07FS	109.19	126.28	96.87
C2	US16DM	108.08	126.54	96.16
C3	US08CS	109.01	121.05	100.68
C4	US14DS	109.73	119.98	102.30
D1	US09GS	110.70	127.16	96.48
D2	UN03ES	107.49	122.21	95.16
D3	US13GS	106.78	117.58	98.70
D4	US17GM	107.13	117.83	89.22

8. REFERENCES

1. Hayes, S. L., 2008, "U3Si2/Al Miniplate Irradiation Test Plan to Support the BFFL Booster Fuel Concept," PLN-2735, February 2008.
2. BFFL Project Personnel, 2008, "BFFL GTL-1 Irradiation Experiment in the Advanced Test Reactor: As-Built Data Package," GTL-1 AS Built, April 2008.
3. Chang, G. S, J. K. Jewell, 2008, "Neutronic Analysis for Final Design of the GTL-1 Experiment Irradiated in ATR South Flux Trap," ECAR-136, August 2008.
4. Moore, G. A., "Fuel Loading Calculations for the GTL-1 Irradiation Experiment," ECAR-164, March 2008.
5. Perez, D. M, G. S. Chang, 2010, "As-Run Neutronics Analysis of the GTL-1 Experiment Irradiated in ATR South Flux Trap," ECAR-1245 Revision 1, July 2011.
6. Wachs, D. M., 2006, "GTL Mini-Plate Experiment Flow Test," EDF-7531, November 2006.
7. Bell, K. J., Albright's Chemical Engineering Handbook, Edited by Lyle F. Albright, CRC Press 2008 p.508.

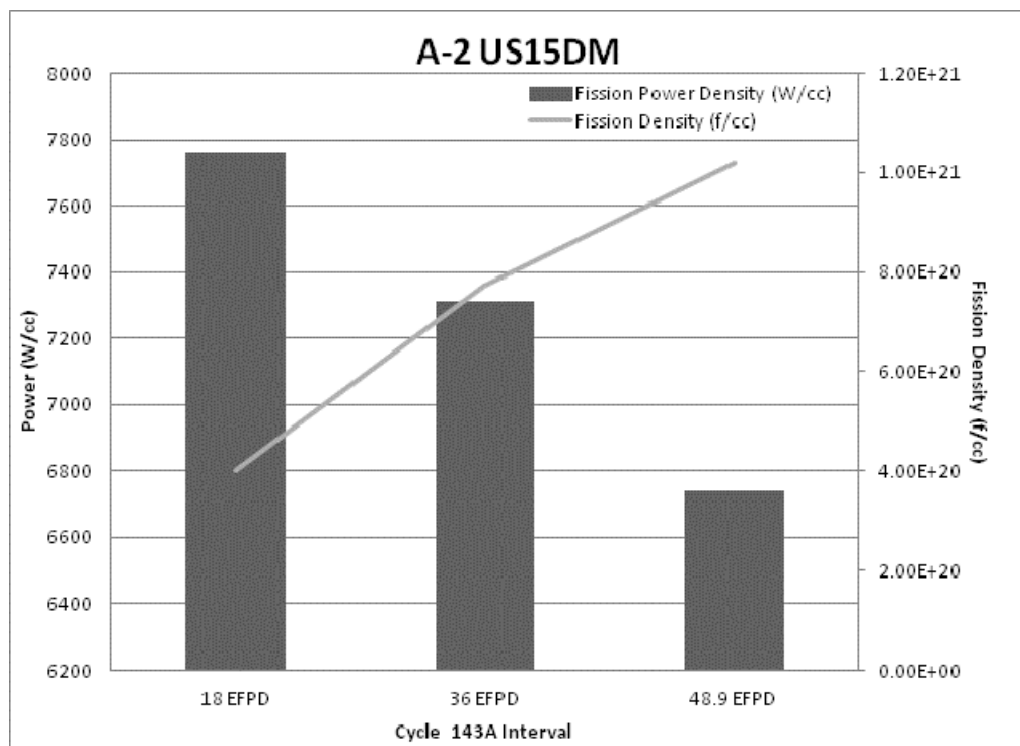
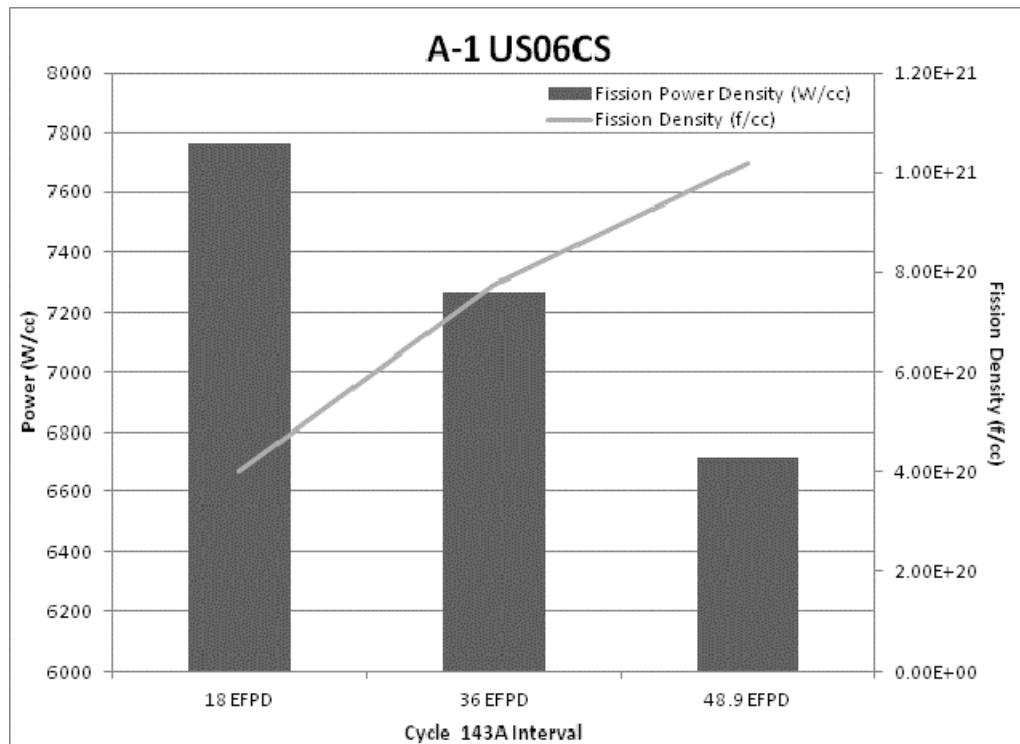
Appendix A

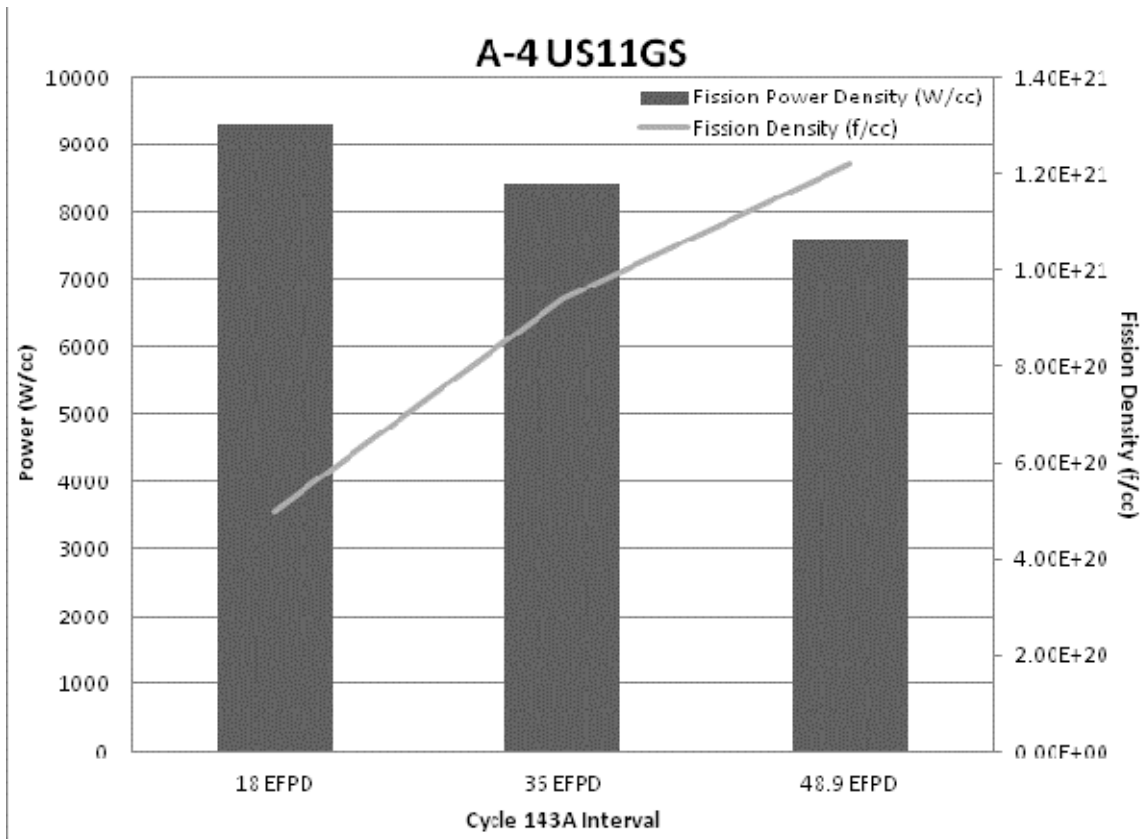
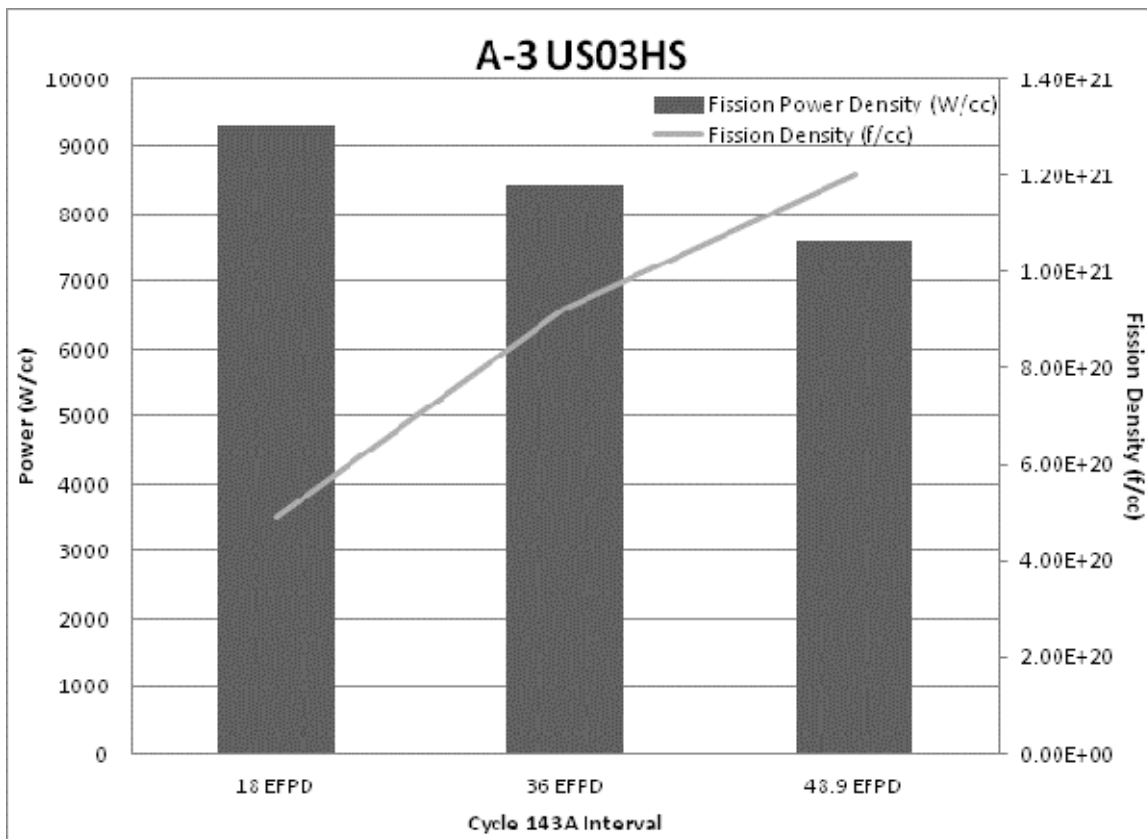
Individual Plate Power and Burnup

Appendix A

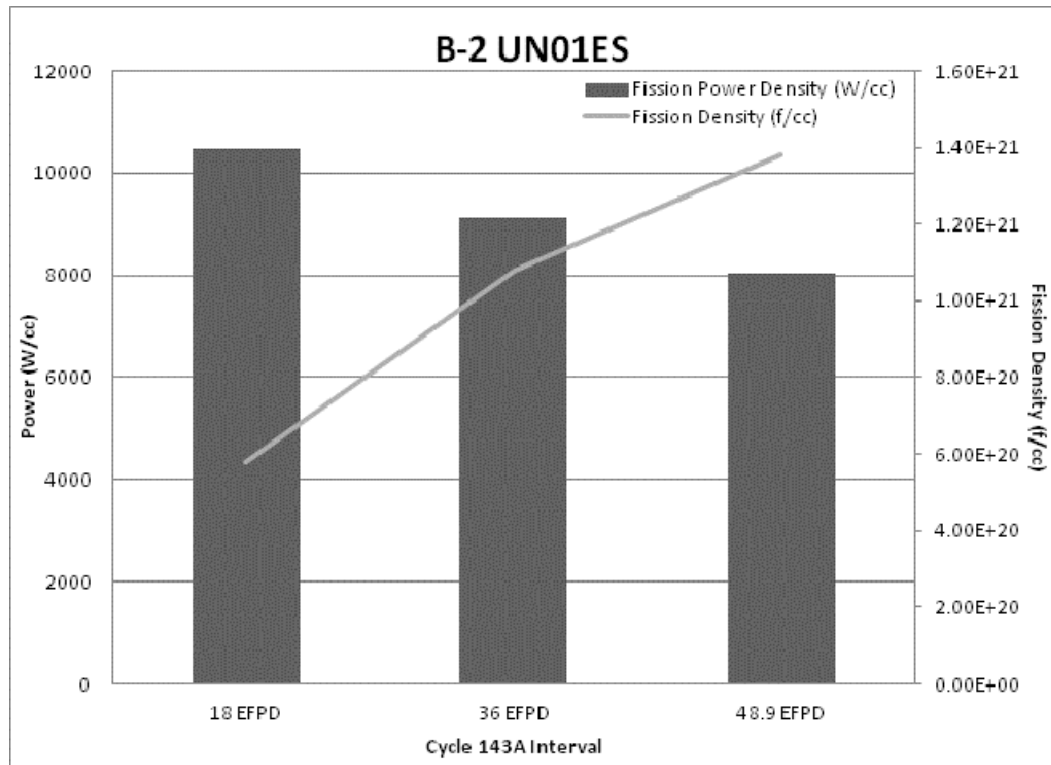
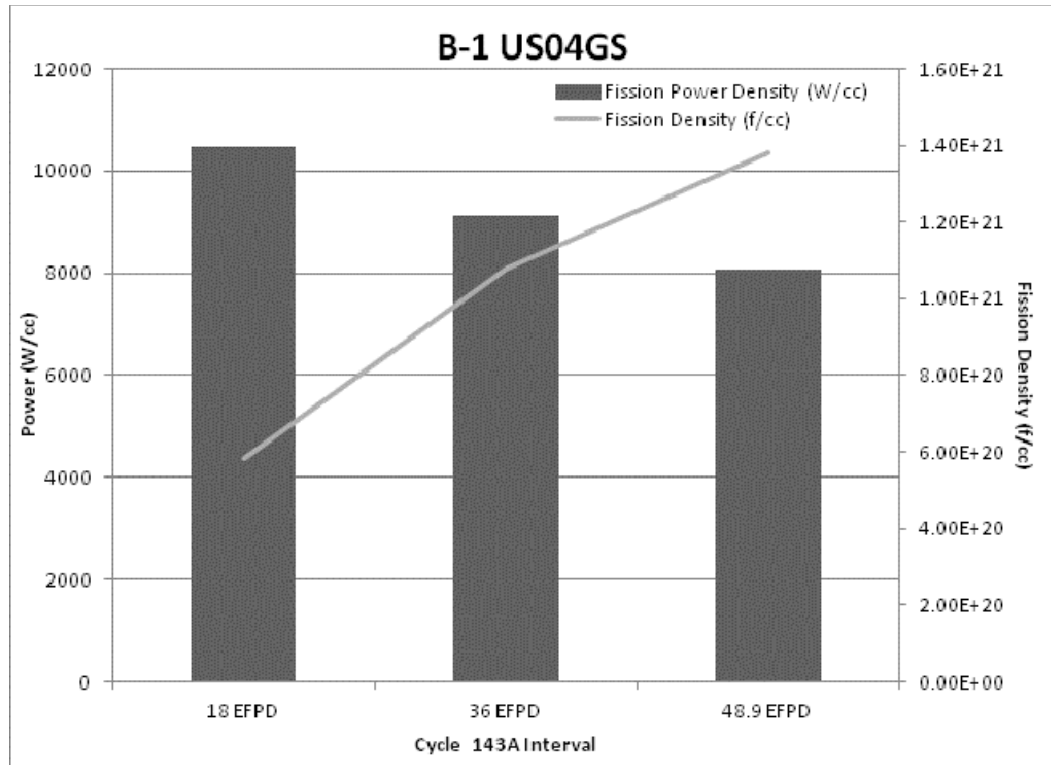
Individual Plate Power and Burnup

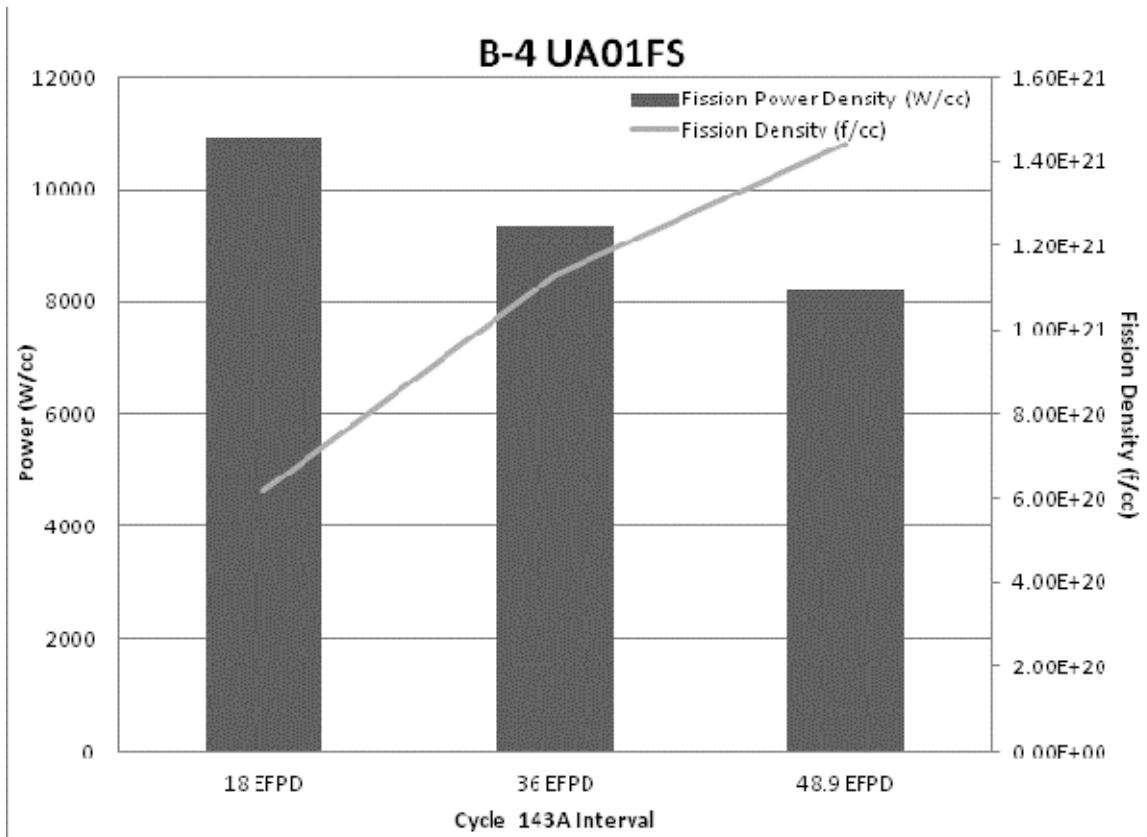
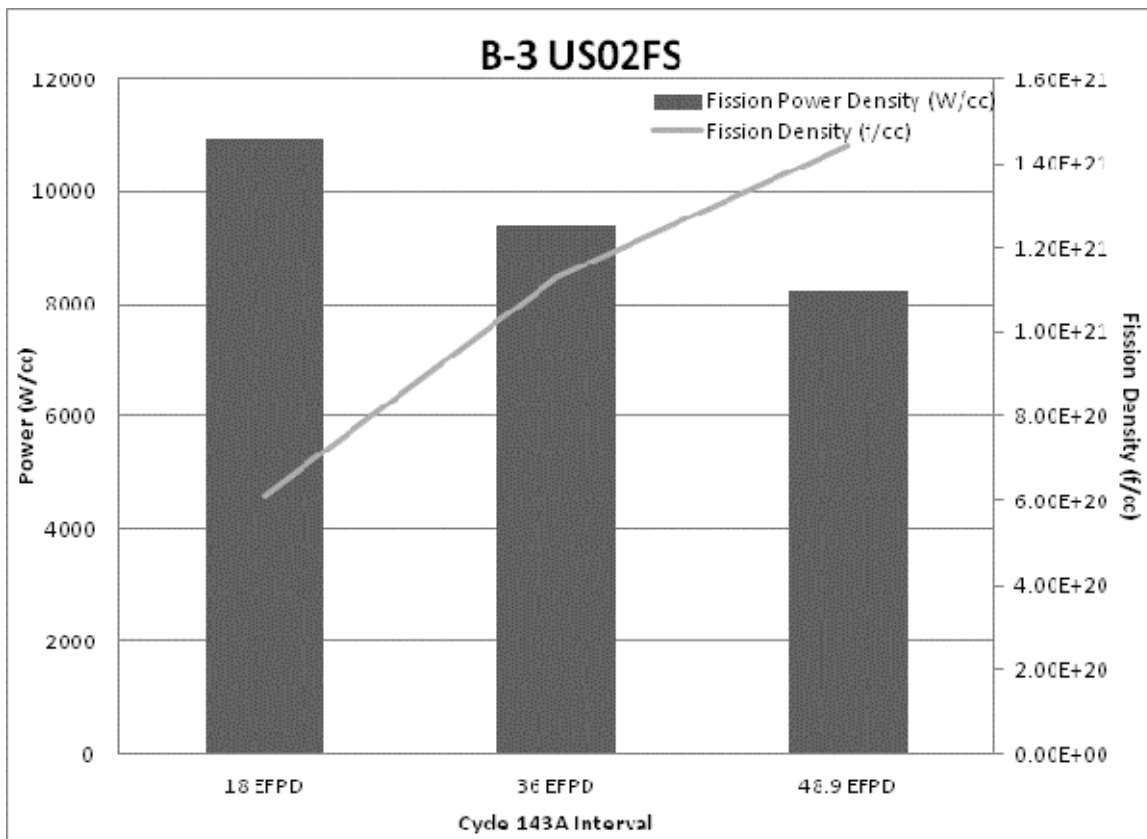
GTL-1 Capsule A



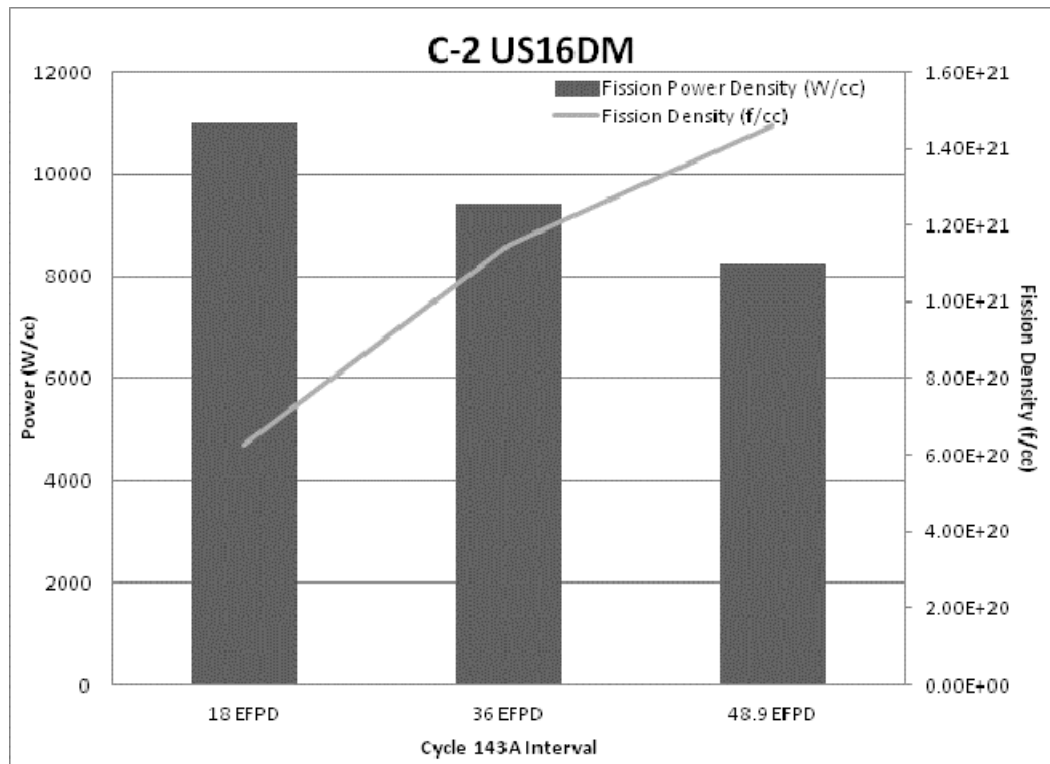
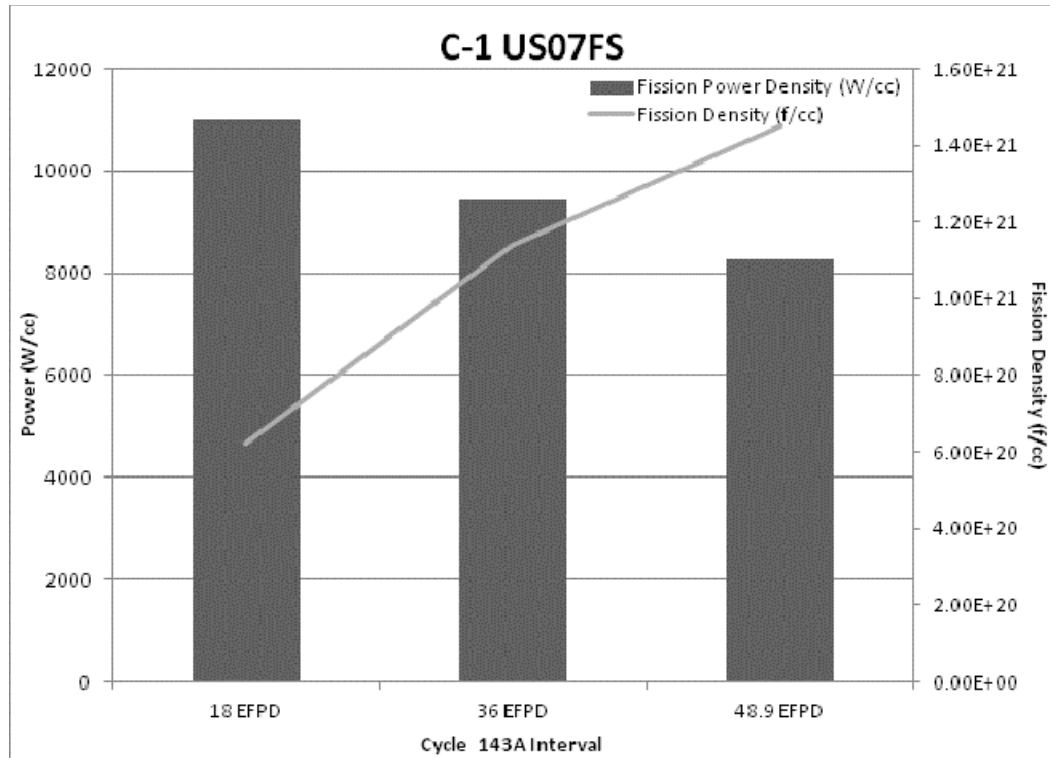


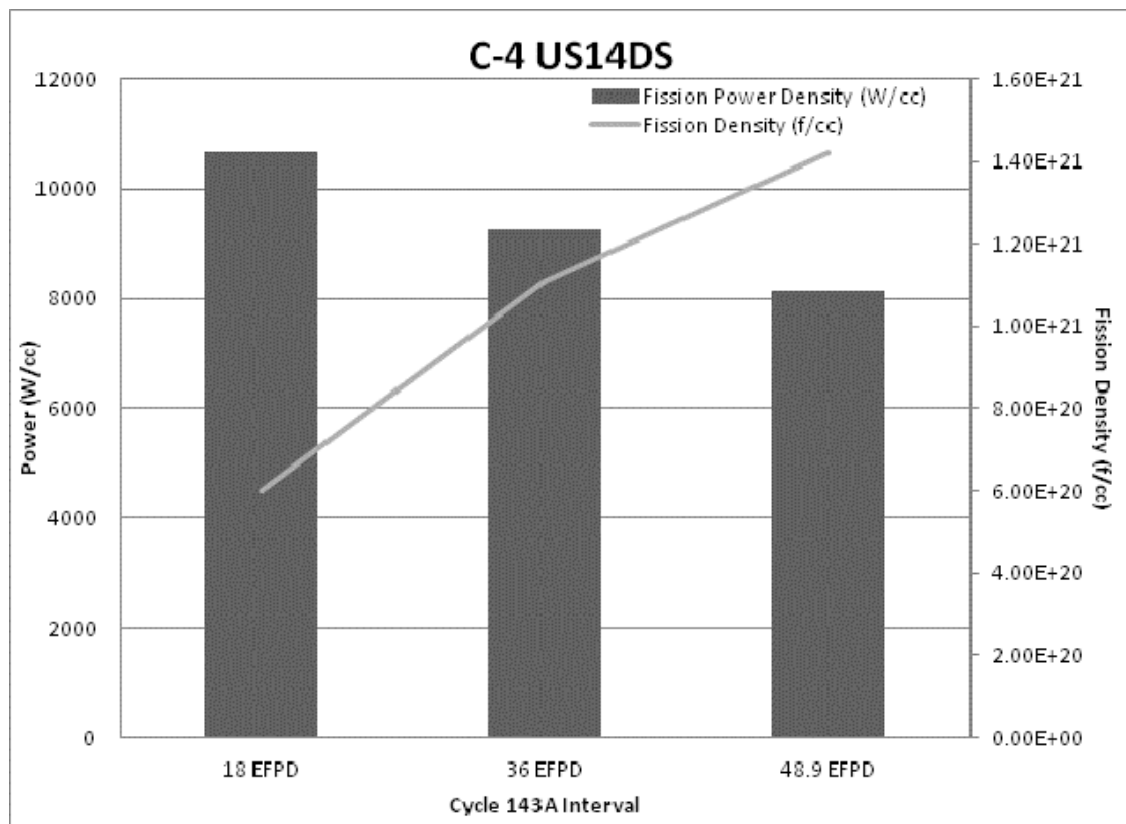
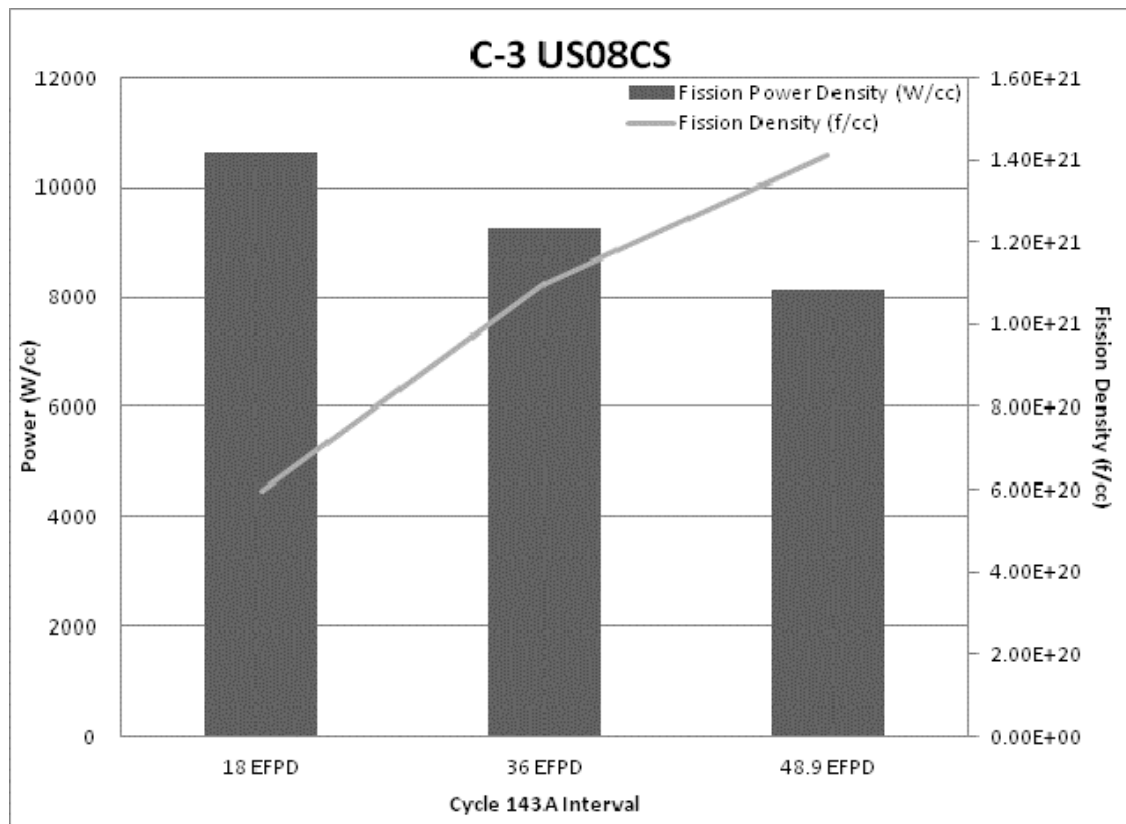
GTL-1 Capsule B





GTL-1 Capsule C





GTL-1 Capsule D

